AU 9011289

UM-P-90/48

QUASICRYSTALLOGRAPHY ON THE SPIRAL OF ARCHIMEDES

by

L. A. Bursill

School of Physics
University of Melbourne
Parkville, 3052, Vic.
Australia

Abstract

The concept of a spiral lattice is discussed. Some examples of known mineral structures, namely clino asbestos, halloysite and cylindrite, are then interpreted in terms of this structural principle. An example of a synthetic sulphide catalyst spiral structure having atomic dimensions is also described. All of these inorganic spiral structures are based on the spiral of Archimedes. The principles for a new type of crystallography, based on the Archimedian spiral, are then presented.

Introduction.

Spiral packings, like the seed arrangements of sunflowers, are interesting because they provide a natural example of living quasicrystals [1]; which lack translational or rotational symmetries yet retain a simple ordering algorithm [2].

The positions of the spiral lattice points may be described using polar coordinates; for example the logarithmic spiral

$$r = AK^{n} \qquad \theta = \phi_d n \qquad [1]$$

where A,K are constants and the integer n labels successive lattice points from the origin out along the generating spiral (Fig. 1). ϕ_d is the divergence angle, i.e. the constant angular displacement between successive lattice points. Spirals following a power law

$$r = an^{k} \qquad \theta = \phi_d n \qquad [2]$$

are also common; for example parabolic (k=0.5) or Archimedian (k= 1).

An analysis of the most efficient disc packings on a parabolic spiral lattice [3], which allows a systematic relaxation of the ideal spiral, showed that the Fibonacci divergence angle ($\phi_d = 2\pi/\tau+1$) is favoured ahead of the Lucas angle ($\phi_d = 2\pi/\tau+3$) or other incommensurate angles $\phi_d = 2\pi/\tau+t$, t=4,5,.... In a subsequent study [4] there was no constraint placed on ϕ_d and discs were allowed to aggregate under a close-packing condition, with successive discs increasing in radius according to a predetermined growth law, for example $R = 0.5n^{b}$,where b was a constant for each packing. The nature of the disc packings was explored for $0<b<1$. It was found that spiral packings were generated, where the divergence angle converged onto the Fibonacci angle 137.508^{o}. Thus it appeared that spiral structures should arise naturally due to close packing of growing discs. Such structures should be no more or less extraordinary than hexagonal close packed arrays of equal discs (k=0 above).

Macroscopic crystallographic studies of sunflowers and other plants, using digitized images and quantitative analyses showed that the power law $r = an^{0.618}$ applied for the sunflower species helianthus tuberosus, whereas a combined logarithmic and power law $r = An^{0.5}K^n$ was required for helianthus annuus [5-9]. Fibonacci angles predominated but Lucas angles occurred with low frequency. Jean [10] has provided a comprehensive and critical review of the subject of phyllotaxis, i.e. the mathematical study of plant geometry and development.

The purpose of this paper is to collect together evidence for inorganic structures which may be described as having a spiral lattice basis, thus identifying a special branch of crystallography. In this way structures which have been regarded hitherto as grossly disordered and rather intractable for analysis may be seen to possess very reasonable chemical and physical principles when referred to a curvilinear basis. The structures of the minerals clino-chrysotile (a variety of asbestos), halloysite and cylindrite are first described. Next some high-resolution images of mixed nickel/tungsten sulphide catalyst particles are presented, which represent a synthetic inorganic spiral lattice structure. Possible growth mechanisms are then discussed briefly. It transpires that all of these structures are best described using the Archimedian spiral $r = an$, with special values for ϕ_d, which are structure dependent. Finally, some general principles of Archimedian spirals, as applied to crystallography, are presented.

Structure of clino-chrysotile asbestos.

The most thorough study of the microstructure of clino-chrysotile is due to Yada [11,12]. Many samples of chrysotile, from diverse localities, including one synthetic sample, were imaged by high-resolution electron microscopy, along directions both parallel and transverse to the fibre axis. Most of the fibrils examined were apparently hollow cylinders, whose circumferential layers formed spiral or even multispiral lattices, as shown schematically in Fig.1. Perfectly

cylindrical layers were also formed with a frequency dependent on the source. Conical fibrils were observed in a synthetic sample. Fibrils greater than about 350Å diameter showed traces of discontinuous growth in two or three steps, depending on growth conditions, and giving rise to various distributions for the fibril diameters. The observations were hindered by electron irradiation damage during observation at the high electron current densities required for high magnification imaging. Thus radiation minimization techniques were necessary.

Yada favoured a structural model for clino-chrysotile in which the a axis is not exactly parallel to the fibre axis and the b axis is not exactly perpendicular to the fibre axis. However, some alternative models, including one polytypic structure which was required to explain some observations, could not be ruled out due to the absence of interpretable two-dimensional HREM images. Details of the cylindrical, spiral and multispiral structures thus remain to be determined. The basic principles of the structures have, nevertheless, been established due to the excellent X-ray diffraction analysis of Whittaker, who first derived the theory for diffraction by a cylindrical lattice [13-24], then analysed the X-ray data to determine the motif which may be assumed to decorate the curved lattice. Bragg and Claringbull [25] and Zussman [26,27] have discussed the structural principles. Individual layers consist of a pseudo-hexagonal network of linked [SiO4] tetrahedra, with approximate parameters a= 5.3A, b= 9.2A (Fig.2a,b). All tetrahedra in the sheet point one way, and joined to it is a brucite (Mg(OH)2) layer in which , on one side only, two out of every three hydroxyls are replaced by apical oxygens of the SiO4 tetrahedra (Fig.2c,d). The perpendicular repeat distance between composite sheets of this type is approx. 7.3A. Pauling predicted in 1930 [28] that a composite sheet, stoichiometry $Mg_3(Si_2O_5)(OH)_4$ with a Si-O layer on one side and a layer resembling brucite on the other would have a strong tendency to curl, because the ideal dimensions of the latter structure are greater than those of the former. Expressing them in a comparable way, they are

Si-O sheet (kaolinite) a =5.16A; b =8.90A

Mg-OH sheet (brucite) a =5.39A; b =9.33A.

There is therefore a strong expansive force on the hydroxyl side tending to make each sheet curl into a cylinder, with the Si-O sheet on the inner side. It thus appears that the relatively weak forces holding the sheets together are insufficient to resist this tendency, and that the structure is a series of such curved sheets stacked on each other, with the tetrahedral component on the inside of the curve. For clino-chrysotile the fibre axis is parallel to the a-axis of 5.3A. Successive sheets remain in register in the a direction, however long the fibre. The relative positions in the b direction of the atoms in neighbouring sheets will vary from point to point along the curve. It follows that the structure can grow indefinitely along the fibre axis, where the structure remains coherent, but extension in the c, or radial, direction is limited, either because the layers are out of step, or because the full circle is completed. Alternatively, if a certain amount of misfit may be tolerated across layers, an Archimedian spiral geometry may be followed (Fig.3) until the misfit is out of range of the energetically tolerable variations in bond length and/or bond angles. Further complexity arises in that the basic layers are actually doubled, c =2x7.3A =14.6A, and there are two symmetrically distinct ways this may be achieved; giving rise to clino- and ortho-chrysotile respectively. The corresponding [010] projections are given as in Bragg and Claringbull [25], Fig.192.. In the common form (clino-chrysotile) successive sheets have the same orietation AAA, whereas in ortho-chrysotile alternate sheets are reversed right and left, in succession ABAB. It must be borne in mind that there is no true unit cell in chrysotile, due to the incommensurate displacement of adjacent layers in the b direction (Fig.3). The orientations of the a, b, c axes with respect to the curved surface of the cylinder are shown in Fig.4a. The a,b dimensions are defined within each sheet, and there is a definite c translation in the b direction of the structure. Within this limitation, the dimensions are, according to Whittaker

	a (A)	b(A)	c(A)	β^o
Clino-chrysotile	5.34	9.2	14.65	$93^o16'$
Ortho-chrysotile	5.34	9.2	14.63	90^o.

Substitution experiments [29 -30] have verified Pauling's predictions: thus replacement of Si by Ge reduces the layer curvature, whereas replacement of Mg by Al, as in the mineral halloysite, results in reversal of the sense of curvature (Fig.4b).

Structure of Halloysite

Electron micrographs of the clay mineral halloysite [31,32,33] show clearly a spiral morphology on the scale of about 0.1um. The local geometry of a kaolinite-like clay layer involved in the halloysite spiral structure [34] is very similar to clino-chrysotile, with Mg2+ replaced by Al3+. Thus, the [SiO4] layer bonds to a modified Gibbsite ($Al(OH)_3$) layer. In the tubular form of halloysite, which is hydrated, the layers are separated by water molecules, giving perpendicular layer spacing 10.25A. In the mineral gibbsite the six hydroxl ions on one side of the unit cell occupy 8.62A, whereas for the Si-O sheet the corresponding six oxygens occupy 8.93A. A hypothetical single unit of kaolinite, free of neighbouring ions , might have a b_o dimension of 8.93A, compatible with the spacing of the oxygen ions on one side and a similar dimension of 8.62A, typical of the hydroxyl ions, on the other. In the hydrated form of halloysite (also known as endellite) the hydroxyl ions are only slightly, if at all, subject to the stretching forces from opposing oxygen layers of the adjacent sheets. The six hydroxyl ions are free to approach their normal spacing of 8.62A while the six oxygens on the opposite side occucpy a distance of 8.93A. Thus, if the vertical bonds remain of equal length relative to each other, a curvature must result, such as that indicated in Fig. 4b. A simple calculation shows that the inner diameter of the resulting cylinder would be 250A, which is the same order as the smallest tubes observed [34]. If the inner

diameter is smaller, the six hydroxyl ions would have to be compressed to occupy a distance less that 8.62A relative to the 8.93A spacing of the oxygen ions. Thus a hollow core, or a highly disordered region, may be expected. For tubes of larger radius of curvature, the OH-OH bonds must stretch. The resultant strain thus finally limits the outer diameter. On dehydration the tubes split and the structure tends to revert to the normal crystalline layer morphology typical of clay.. Kirkman's images [33] show a tendency of the tubular layer structure of halloysite to shread into packets of concentric layers, with some evidence for polygonalization of the cross-section, giving a "multifaceted squat cylinder" [33].

Structure of cylindrite.

Cylindrite forms macroscopic cylinders (Fig.5a) and its growthproceeds apparently by an endless lateral advance in the tangential direction of layers enveloping the cylinders [41]. In cross-section they form an irregular Archimedian spiral (Fig. 5a). This is a layer structure, analogous to clino-chrysotile, where the layers curls up into a cylinder, but with much larger radius of curvature, 1mm rather than a few 100A. Hence on the HREM scale the layers are almost flat (see Fig.5b and [35]). In another variant of the structure the layers are sinusoidally corrugated (see Fig. 5c and [35]). Towards the centres of the cylinders the layers cannot adapt to the increased curvature and drastic deformation and twinning occur[36]. Most of what is known about the mineralogy, chemistry and crystallography of cylindrite is due to Makovicky [37-41]. Cylindrite approximates to the formula $FePb_3Sn_4Sb_2S_{14}$ with minor Ag. It is composed of two sets of alternating layers(Fig. 5d). One set, based on a pseudo tetragonal sub-cell, and referred to as T below, has approx. stoichiometry $(Pb,Ag)_{14.3}Sn_{5.7}Sb_{4.4}Fe_{1.6}S_{26}$, which are (100) slices, two atom layers thick, of a deformed PbS (galena or NaCl-type) structure (see Fig. 5d). The other, based on a pseudo-hexagonal subcell, and referred to as O below, consists of layers of approx. $Sn_{6.2}Sb_{2.3}Fe_{1.5}S_{24}$; which are essentially (001) slices of SnS_2, or $Cd(OH)_2$-type,

structure one octahedron, or three atomic layers thick (see Fig. 5d). The Sb and Fe atoms are situated at steps (Fig. 5d), causing layer corrugations. The layer stacking direction is a* = a and the bounding surfaces of the layers are (100). In the T layers these surfaces contain equal numbers of cations and anions, arranged on approx. square nets; but in the O layers they contain only anions, arranged in approx. triangular nets.

The unit mesh parameters are [40] T:a_T = 11.733, b_T = 5.790, c_T = 5.810A; $\alpha_T = 90.00^o$, $\beta_T = 92.38^o$, $\gamma_T = 93.87^o$ and O:a_O = 11.709, b_O = 3.670, c_O = 6.320A; $\alpha_O = 90.00^o$, $\beta_O = 92.58^o$, $\gamma_O = 90.85^o$. Note the small divergence betwen stacking vectors a_T and a_O, as well as their β and γ values. The PbS pseudocell of T has an axis about 12% larger than that of the corresponding pseudocell of O. This is consistent with the former being rich in Pb2+ and the latter in Sn4+, with ideal bond lengths to S of 2.947 and 2.549A respectively. The unit cell axes are related to the morphology of cylindrite as follows: the cylinder axis is close to $c_T = c_O$; the layer stacking direction a* is parallel to a radius of the cylinder, and therefore ranges in direction through 360^o and the remaining vector $b_T = b_O$ is at right angles to both of these; i.e. approx. tangential to the cylinder, and therefore also ranging in direction by 360^o [35,36].

An exhaustive HREM study by Williams and Hyde [36] revealed further fine details of structural modulations and steps, as well as intergrowth defects. It should be clear from Fig. 5b that the structure is approximately periodic parallel to the b axis but sighting perpendicular to the layers shows variable lattice fringes, giving the appearance of gross disorder (cf. also Fig. 3). Williams and Hyde [36] have modelled the structure of the corrugated variant (Fig. 5c) but it remains to explain the details of the cylindrite structure reepresented by our Fig. 5b. Further work on this problem has begun in our laboratory using computer-simulated images and spiral lattice models, like Fig. 3, to interpret the HREM images. It is important to determine how perfectly or imperfectly the spiral lattice model may be reached in reality. It seems likely that locally-relaxed

crystallographic structures may occur, whereas the overall geometry is best described as spiral.

Embryonic spiral structures on sulphide catalysts.**

Fig. 6a,b shows two examples of nickel/tungsten sulphide catalyst particles. Note the NiS core, which appears to be multiply-twinned. The aim of the preparative work was to induce a monolayer coating of WS_2, in order to optimize the surface exposure of the latter and hence enhance the catalytic properties. In the examples shown the monolayer has already started to wrap around the NiS core, producing an elementary spiral of WS_2. This example may be important because it illustrates one of the possible growth mechanisms for such structures. In fact the spiral is not a perfect Archimedian form, being to some extent polygonalized due to the shape of the underlying crystalline core. Clearly, this observation confirms that synthetic spirals may be produced on the scale of atomic dimensions. Further attempts to produce novel spiral structures, using chemical as well as physical principles, are progressing.

Along one side of Fig. 6b areas of two-dimensional fringes were obtained. Close inspection reveals that the fringe spacing is constant within the WS_2 layers (3.7A) but these short fringes run discontinuously from layer to layer, as expected, since the layer curvature leads to incommensurate alignment of adjacent layers, as was the case for all the mineral species described above.

Discussion.

(a) Basic geometry. Jagodzinski and Kunze [42] described two basic spiral configurations, in connection to chrysotile; the simple cylindrical helix (Fig. 7a) and the simple Archimedian spiral (Fig. 7b). The steps (arrowed) indicate schematically how additional unit motifs may be added, implying growth

** The specimen was prepared at the Institut du Catalayse, Universite de Lyon 1, and the microscope observations were made in 1987 with Drs. Christian, Galezot and Blanchin, in Lyon, at the Department de Physique des Materiaux.

mechanisms. Also shown in Fig. 7c is a combined helix/spiral which is, of course, the more general combination. Coherency or incommensurability relationships may be derived for an arbitrary two-dimensional lattice by drawing a number of repetitions in plane format, and then simply rolling it up around the desired axis (see Figs. 3 and 8).

(b) Multi-layer spirals. Because the structure of chrysotile and cylindrite contain two layers in the unit cell, then there should be two interleaved spirals. The model preferred by Whittaker [21] for chrysotile is based on a double-spiral, imposing a two-fold rotational symmetry on the generating spiral. Single and double spiral bases are compared in Fig. 8a,b. In his study of chrysotile Yada [11,12] found evidence for circular (cylindrical), as well as single, double and multiple-spiral variants. Such behaviour is indicative of polytypic formation. Unfortunately, the resolution of his images was not sufficient to allow the local structures to be determined by image simulation and matching. The HREM images of cylindrite (Fig. 5b) often show a multi-layer structure. These latter images have not yet been interpreted satisfactorily in terms of a full crystallographic model.

Fig. 8 shows how single, double, three-fold and six-fold spirals may arise due to wrapping, for example, simple cubic AAAA..., hexagonal ABAB... ,face-centred cubic ABCABC... or the polytype ABCDEFA... layer packings about a spiral axis. Note that an N-layer stacking transforms into an N-fold spiral containing N arms separated by $2\pi/N$ radians.

(c) Symmetry restrictions.

It is now apparent that there exists, in principle, an interesting crystallography based upon the Archimedian spiral. Whittaker [18] has already introduced a classification of cylindrical lattices, including helical and spiral cases, in order to make a quantitative study of the diffraction patterns of

chrysotile. His analysis is included here for completeness. Although derived with the study of chrysotile in mind, in fact it should be applicable to all of the structures described above.

(i) Axial parameters. The axial parameters are taken[18] as follows:

a' is the normal spacing between each successive pair of cylindrical or spiral surfaces,

b, c are the lattice parameters of the two-dimensional lattice (the generating lattice) where c is taken as the axis which is more nearly parallel to the cylinder axis,

α is the angle included between the b and c axes,

β is the angle such that each successive two-dimensional lattice is displaced by a distance $a'\cot\beta$, parallel to the cylinder axis, with respect to its inner neighbour. It is convenient to put $a = a'\operatorname{cosec}\beta$.

(ii) Possible types of spiral cylindrical lattices [18]. Assume first that the b axis lies on a right section of the cylinder. It then follows that $\beta = \pi/2$, since the successive turns of the spiral formed by the b axis of the generating lattic are coplanar. There are, therefore, only two possible regular lattice types in these circumstances, which may be named as follows

Type I Monoclinic $\alpha \neq \beta = \pi/2$, and

Type ii Orthorhombic $\alpha = \beta = \pi/2$.

No relationship between the lattice parameters is imposed by the construction of a spiral cylindrical lattice.

If the b axis does not lie on a right section of the cylinder then it follows that $\beta \neq \pi/2$ and the b axis must advance a distance $a'\cot\beta$ along the cylinder axis for every turn of the spiral. b must therefore be inclined to the right section of the cylinder at any given point of the cylinder at an angle given by $\sin\delta = a'\cot\beta/2\pi\rho$, where ρ is the radius of curvature of the cylinder at that point. This

clearly varies continuously along the b axis, so that either the axes of the generating lattice must be curved, or the angle β must vary throughout the lattice. However, the distortions involved may be very small in practical cases. For example, in chrysotile the maximum curvature required in the generating lattice would involve a total change of direction throughout the lattice of about 10', although the corresponding variation in β if the b axis of the generating lattice were straight would be of the order of 5^{o}. Thus the necessarily slightly imperfect helical spiral cylindrical lattices of the following types may also be of practical interest:

Type III Anorthic $\alpha \neq \beta \neq \pi/2$

Type IV Monoclinic $\beta \neq \alpha = \pi/2$.

(iii) Cylindrical projections [18]. It is evident that a spiral layer structure can only be formed if the individual layers have dissimilar sides, and the successive layers have negligible steric interactions with one another. It follows that in such a structure these layers constitute zones lying between parallel circular or spiral cylindrical surfaces within which the structure remains coherent. If any intensive property of the structure (e.g. electron density) is integrated along the normals to these surfaces over the thickness of the layer and projected onto the neutral surface of the layer with respect to bending, then the two-dimensional projection so obtained will form a regular repeating pattern. It may be conveniently described as the cylindrical projection onto (100), by analogy with normal crystallographic literature. This projection is based on the generating lattice of the structure, although the different layers themselves differ from one another in detail as a result of their different curvatures. A second regular projection may be defined as follows. Take any plane orthogonal to the cylindrical surfaces of the lattice. From every point on this plane construct an arc parallel to the b axis which lies within the same layer. Continue each arc until a point is reached whose environment in the cylindrical surface is identical with that of the

starting point of the arc. If any intensive property of the structure is summed and projected along the arc onto the initial plane then a two-dimensional repeating pattern is obtained. This pattern lies on a lattice with parameters a, $c\sin(\alpha + \delta)$ and included angle β. It may conveniently be described as the cylindrical projection down (010).

The cylindrical projection on (100) may have any of the two-dimensional space groups belonging to the oblique and rectangular systems. But, because the inside and outside of the layer must be dissimilar, it is not permissible for the cylindrical projection down [010] to contain either a two-fold rotation point or a symmetry line perpendicular to the a axis. Therefore, the only permissible two-dimensional space groups for the projection are p1, pm, pg and cm, in the usual notation (International Tables for Crystallography, [43]), and their orientations are subject to restrictions. In order to make the latter clear it is convenient to use full space group symbols with the same conventions as to the order of the symbols as in the three-dimensional orthorhombic space groups, and to use a and b to denote centred lattices on the projections of (100) and down (010) respectively. The notation of these possible space groups, in the latter projection, is then p11, p11m, p11g, and b11m. The alternative orientations pm11, pg11,and bm11 are not permitted.

(iv) Centred spiral cylindrical lattices [18] In spiral lattices which have a rectangular generating lattice (all those with $\alpha = \pi/2$) the latter may be primitive (p) or centred (c). A second type of lattice analogous to a centred lattice arises if one or more sets of similar cylindrical lattice layers are intercalated between those which define the repeating unit in the radial direction. Such intercalated sets of layers constitute coaxial spiral lattices having the same parameters a, b, c, α and β, but having different values of a_0 and relative displacements parallel to the cylinder axis. Some examples were referred to above, see discussion of multi-

spirals. Such composite lattices may be denoted by cn, if the intercalated layers divide the a' spacing into equal parts.

(d) Pseudosymmetric n-fold axes for special axial ratios. For the case of cylindrical lattices, let it be assumed that the b axis lies in a right section of the cylinder. It then follows that there is a relation between a and b for such lattices which is necessary for their existance, namely

$$nb = 2\pi a' \quad (n \text{ integer})$$

This ensures that there is an integral number of b units on every layer provided that there is an integral number on any one layer.

For the special case of chrysotile asbestos the axial ratio a'/b = 14.65/9.2 = 1.59, implying n = 10. Thus, the reciprocal lattice section normal to the cylinder axis should exhibit 10-fold rotational symmetry. It is remarkable that Whittaker published simulated diffraction patterns, obtained using an optical diffractometer, which indeed exhibited this symmetry (Whittaker, [22]). Thus chrysotile rightly belongs to the more recently defined class of structures now known as decagonal quasicrystals (Steinhart and Ostlund [44]).

This special axial ratio a'/b = 10 is perhaps not sufficiently stressed by Whittaker. In fact, the more typical case must be that of the spiral lattice. Plotting the corresponding spiral lattice, using the same axial ratio, gives the very interesting pattern shown in Fig. 3. Note the pseudo-symmetric 10-fold axis. Thus a pseudo n-fold axis is possible whenever one additional unit cell is inserted in each of n quadrants subtending angle $2\pi/n$ at the centre (n= 10 for chrysotile). Thus ten almost identical segments arise, closely-ressembling a decagonally-twinned crystal in this projection. In general, however, the spiral geometry should predominate, since is most unlikely that the axial ratio will be exactly $n/2\pi$. Of interest to quasicrystallographers is the possibility of filling the plane, with almost identical structural units of one type only, with the potential of yielding any n-fold rotational symmetry. This adds a new twist to tiling the plane!

(e) Spiral lattices and dislocations. Jagodzinski and Kunze [42] pointed out that spiral and helical cylindrical structres may be described in terms of radial and axial dislocations. Whittaker [18] then showed that it is possible to give a formal description of all the cylindrical lattices in terms of dislocations introduced into a normal three-dimensional lattice of appropriate dimensions. Thus a regular circular cylindrical lattice may be considered to arise by the introduction of regularly spaced edge dislocations of Burgers vector **b** parallel to the cylinder axis, with a density a'/bρ in the layer of radius ρ (a' is the normal layer spacing and b is an axis lying within a layer, being almost normal to the cylinder axis. Such a lattice may then be converted to a regular spiral by introduction of a Volterra screw dislocation along the axis with Burgers vector Nt. Sighting along radial lines in Fig. 3 or Fig.5b reveals apparently the edge dislocations. However these descriptions are purely formal. It is not supposed that the lattice is stressed in the usual way by such dislocations; rather it it the **unstressed curved** shapes of the structural elements that leads to the spiral or cylindrical structures, as predicted by Pauling. Thus the concept of a spiral cylindrical lattice, including helical and cylindrical special cases, would appear to be the preferred mathematical basis, rather than make reference to a dislocated normal three-dimensional lattice. Of course, that is not to exclude dislocations and stacking disorders with their normal significance as lattice defects. These may readily be introduced into spiral structures, as shown already by Williams and Hyde [36]. For example; (i) a radial screw dislocation would involve a join between a circular and a spiral cylindrical lattice; (ii) a screw dislocation parallel to the cylinder axis but not along it would introduce a measure of helical structure in a regular cylindrical lattice without converting it into a helical lattice, and would thus produce a longitudinal growth mechanism for a regular cylindrical lattice; and (iii) radial edge dislocations with Burgers vector **b** could convert spiral lattices

into tapering or conical structures. In fact Yada's high-resolution images show a variety of irregular spiral forms in asbestos.

(f) Spiral to normal crystal phase transition. It was noted above, in reference to halloysite, that the electron microscope images showed a segmented, or polgonalized texture. It appears that, in that case, the structure first grew as a spiral lattice and then shreaded as it transformed into the polygonal form. It seems likely that this was due to dehydration, i.e. loss of water from between the kaolinite layers, which may occur either naturally, on weathering, or else simply on observation in the electron microscope under vacuum. Perhaps more fundamentally, it is conceivable that the spiral to normal crystal transformation may also occur under external uniaxial or shear stress, or simply when the radius of curvature of the spiral becomes either too large or too small, when the two components whose lattice misfit induces the curvature may then adopt a corrugated or modulated structure, as occurred for cylindrite, or some other crystalline form having a normal crystallographic space group. We have observed a wide variety of textures in cylindrite specimens, as did Williams and Hyde and Makovicky, as might be expected for such an unusual mineral phase.

(g) Synthetic spiral structures. The example of tungsten sulphide on a nickel sulphide substrate, referred to above, which shows the begining of a spiral morphology, is important because it implies that it is quite realistic to expect that novel spiral crystals may be produced by design. Of course sythetic asbestos has been used commercially for many years. The principles made evident above should be useful for design of new phases, for example using crystalline or amorphous whiskers as a rotating substrate and depositing multilayers of different chemical species, either from solution or from the vapour phase. Spiral crystals should also show a strong tendency to accept intercalated layers which may impose interesting physical and chemical properties. It is also reasonable to

suggest that spiral arrays of electronic components may sometimes offer more efficient decign geometries than traditional square arrays cf. [45].

Conclusion.

The above review of old and new spiral structures based on the spiral of Archimedes should renew interest in mineral structures as well as point to new synthetic routes for the growth of new types of quasicrystalline materials, which are fascinating from both theoretical and technological points of view. Given the known effects of asbestos on the lungs, it may be necessary to take care in handling the nanocrystalline forms.

Acknowledgements.

This work was supported financially by the Australian Research Council, the Victorian State Government and the University of Melbourne. The author thanks Peng Ju Lin for Figs. 5a,b,c and Fan XuDong for the spiral graphics (Fig. 3).

References.

[1] N. Rivier, J. de Physique, 47, (1986) C3-299.

[2] L.A.Bursill, Peng Julin and Fan XuDong, Modern Physics Letters B1, (1987) 195-206.

[3] Fan XuDong, L.A.Bursill, Peng JuLin, Mod. Phys. Letts. B3 (1989) 119-124

[4] L.A.Bursill and Fan XuDong, Mod. Phys. Letts. B2 (1988) 1245-1252.

[5] Fan XuDong, Peng JuLin and L.A.Bursill, Inter.J.Mod. Phys. 2 (1988) 121-129.

[6] Fan XuDong, L.A.Bursill and Peng JuLin, Inter.J.Mod.Phys. B2, (1988) 131-146.

[7] L.A.Bursill, George Ryan, Fan XuDong, J.L.Rouse, Peng JuLin and Ann Perkins, Mod.Phys.Letts. B3, (1989) 1071-1085.

[8] George Ryan, J.L.Rouse and L.A.Bursill, J.Theor. Biol., in press (1990).

[9] L.A.Bursill, J.L.Rouse and Alun Needham, Symmetry, in press (1990).

[10] R.V.Jean "Mathematical Approach to Pattern and Form in Plant Growth" J.Wiley. NY. 1984.

[11] K.Yada, "Study of Chrysotile Asbestos by a High-Resolution Electron Microscope", Acta Crystallogr. 23, (1967) 704-707.

[12] K.Yada, "Study of Microstructure oif Chrysotile Asbestos by High-Resolution Electron Microscopy", Acta Crystallogr. A27, (1971) 659-664

[13] E.J.W.Whittaker "An orthorhombric variety of chrysotile", Acta Cryst. 4, (1951) 187.

[14] E.J.W.Whittaker, "The Structure of Chrysotile" Acta Cryst. 6, (1953) 747-748

[15] E.J.W.Whittaker, "The Diffraction of X-rays by a Cylindrical Lattice I", Acta Cryst. 7, (1954) 827-832

[16] E.J.W.Whittaker, "The Diffraction of X-rays by a Cylindrical Lattice II", Acta Cryst. 8, (1955) 261-265.

[17] E.J.W.Whittaker "The Diffraction of X-rays by a Cylindrical Lattice III", Acta Cryst. 8, (1955) 265-271.

[18] E.J.W.Whittaker, "A Classiciation of Cylindrical Lattices", Acta Cryst. 8, (1955) 571-574.

[19] E.J.W.Whittaker, "The Diffraction of X-rays by a Clindirical Lattice IV", Acta Cryst. 8, (1955) 726.

[20] E.J.W.Whittakjer and J.Zussman, "The Characterization of Supertime Minerals by X-ray diffraction", Mineral.Mag. 31, (1956) 107-126.

[21] E.J.W.Whittaker, "The Structure of Chrysotile II, Clino-Chrysotile", Acta Cryst. 9 (1956) 855-862.

[22] E.J.W.Whittaker, "The Structure of Chrysotile III, Ortho. Chrysotile", Acta Cryst. 9 (1956) 862-864.

[23] E.J.W.Whittaker, "The Structure of Chrysotile IV, Para-Chrysotile", Acta Cryst. 9 (1956) 865-867.

[24] E.J.W.Whittaker, "The Structure of Chrysotile V, Diffuse Reflexions and Fibre Texture", Acta Cryst. 10, (1957) 149-156.

[25] W.L.Bragg and G.F. Claringbull "Crystal Structures of Minerals", London, G.Bell (1965) pp282-287.

[26] J.Zussman, G.W.Brindlay and J.J.Comer "Electron Diffraction Studies of Supentric Minerals", Amer. Mineral 42, (1957) 132-153.

[27] W.A.Deer, R.A.Howie and J.Zussman, "An Introduction to the Pock-Forning Minerals", Longman (1970) pp242-250.

[28] Linus Pauling, "The Structure of the Chlovites", Proc. Nat.Acad.Sci. 16 (1930) 578-582.

[29] N.L.Bown and O.F.Tuttle, "The System MgO-SiO_2-H_2O", Bull. Geol.Soc.Amer. 60 (1959) 439-460

[30] D.M.Roy and R.Roy "An Experimental Study of the Formation and Properties of Synthetic Serpentines and Related Layer Silicate Minerals", Amer.Miner. 39, (1959) 957-975

[31] J.B.Dixon and T.R.McKee "Internal and External Morphology of Tubular and Spherovdal Halloysite Particles", Clays and Clay Minerals 22 (1974) 127-137

[32] J.H.Kirkman, "Possible Structure of Halloysite Disks and Cylinders Observed in Some New England Rhyolitic Tephras", Clay Minerals 12 (1977) 199-216

[33] J.H.Kirkman, "Morphology and Structure of Halloysite in New Zealand Tephras", Clays and Clay Minerals 29 (1981) 1-9.

[34] T.F.Bates, F.A.Hildebrand and A.Swineford, "Morphology and Structure of Endellite and Halloysite", Amer.Mineral 35 (1950) 463-484

[35] J.Barbier, K.Hiraga, L.C.Otero-Diaz, T.J.White, T.B.Williams and B.G.Hyde "Electron Microscopic Studies of Some Inorganic and Mineral Oxide and Sulphide Systems", Ultramicros. 18 (1985) 211-234

[36] T.B.Williams and B.G.Hyde "Electron Microscopy of Cylindrite and Frankeite", Phys. Chem.Minerals 15 (1988) 521-544.

[37] E.Makovicky, "Cylindrite-Crystallography and Crystal Chemistry", Amer.Mineral. 56 (1971) 353 (Abst.).

[38] E. Makovicky "Microstructure of cylindrite" Neues Johrbuch für Mineral. Monatshetie (1971) pp404-413

[39] E.Makovicky "Mineralogical data on cylindrite and incaite" Neues Jb. Miner.Mh. (1974) pp235-256

[40] E.Makovicky "Crystallography of Cylindrite, Part I: Crystal Lattices of Cylindrite and Incaite" Neues Jb.Mineral Abhandlungen 126 (1976) 304-326

[41] E.Makavicky and B.G.Hyde "Non-Commensurate (Misfit) Layer Structures" Struct.Bonding 46 (1981) 100-170.

[42] H.Jagodzinski and G.Kunze "Die Rollchemstruktur des Chrysotils III Verselzungswachsturm der Röllchen". Neues Jb. Mineral. Monatschefte (1954) 137-150.

[43] T. Hahn (Ed.) "International Tables for Crystallography: Vol.A: Space Group Symmetry", D.Reidel, Dordrecht (1983).

[44] P.J.Steinhardt and S. Ostlund, "The Physics of Quasicrystals", World-Scientific, Singapore (1987).

[45] M.J. Blum, M. Braum and D. Rosenfeld "Fast magnetic resonance imaging using spiral trajectories" Austral.Physical and Engineering Sciences in Medicine 10 (1987) 79-87.

Figure Captions.

Figure 1: Schematic representation of the spiral (a), multispiral (b) and cylindrical (c) morphologies observed by Yada for asbestos. The dotted circles represent the outside diameter of the fibrils (i.e. approx. 200A).

Figure 2: Brucite, $Mg(OH)_2$, and silica tetrahedral [SiO_4] sheets comprising the structure of asbestos, for [001] and [100] projections.

Figure 3: Arrangement of structural units on an Archimedian spiral. Note that there is no true unit cell repetition: both the angles and edges of each unit are different. Periodic translation vectors can only be retained parallel to the cylinder axis.

Figure 4: (a) Orientation of a, b, c axes of asbestos relative to the curved surface of a cylinder. (b)Relationship between sense of curvature of misfit sheets of chrysotile (Mg,Si), synthetic clay (Ge,Mg) and halloysite (Si,Aℓ) respectively.

Figure 5: (a) Scanning electron micrograph of cylindrite looking approximately along the cylinder axis. Note the distinct spiral growth morphology (cf. [41]) outer diameter approx. 1mm.(b)HREM image of cylindrite obtained from a cross-section of Fig. 5a. Note that the layers are approximately flat on this scale. Sighting approximately normal to the layers, at glancing angle, reveals an apparently disordered structure. (c) HREM of the same cylindrite specimen showing an area of a variant sinusoidally-modulated structure (serpentine).(d)Representation of T (PbS type) and O (Cd(OH)2 type) sheets of cylindrite. Mismatch of the c parameters of

these two sheets leads to the curved layers of cylindrite.

Figure 6: Two examples (a,b) of nickel sulphide core structures around which tungsten sulphide sheets have been wrapped, forming essentially an elementary spiral structure, albeit with irregular cross-sections.

Figure 7: Planar spiral (a) and helical spiral (b) configurations formed by rolling up two-dimensional sheets. (c) Shows a combined helix/spiral. Growth steps are arrowed.

Figure 8: Single, double, three-fold and six-fold spirals due to wrapping, for example, simple cubic (AAA....), hexagonal (AB AB AB.....), face centred cubic (ABC ABC....) or polytype (ABCDEFA.....) layer packings about a spiral axis.

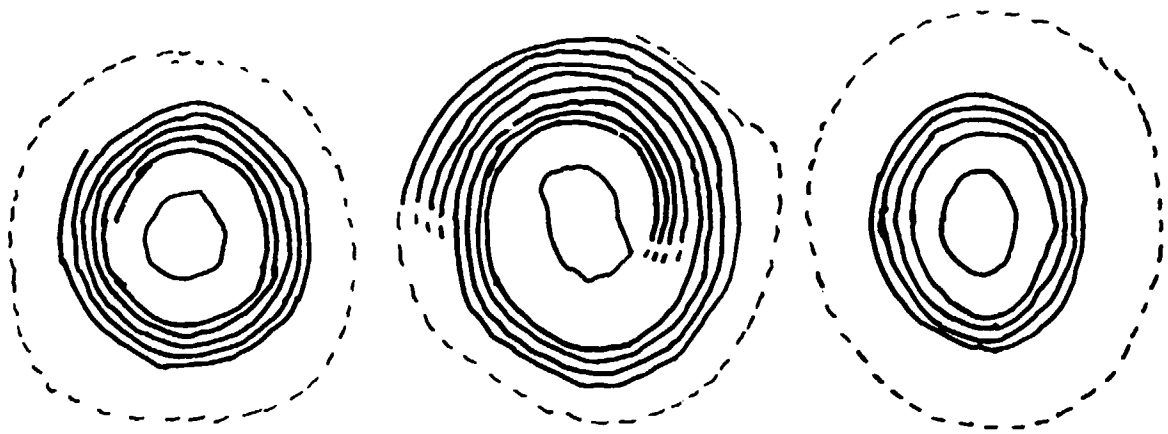

a b c

Fig 1

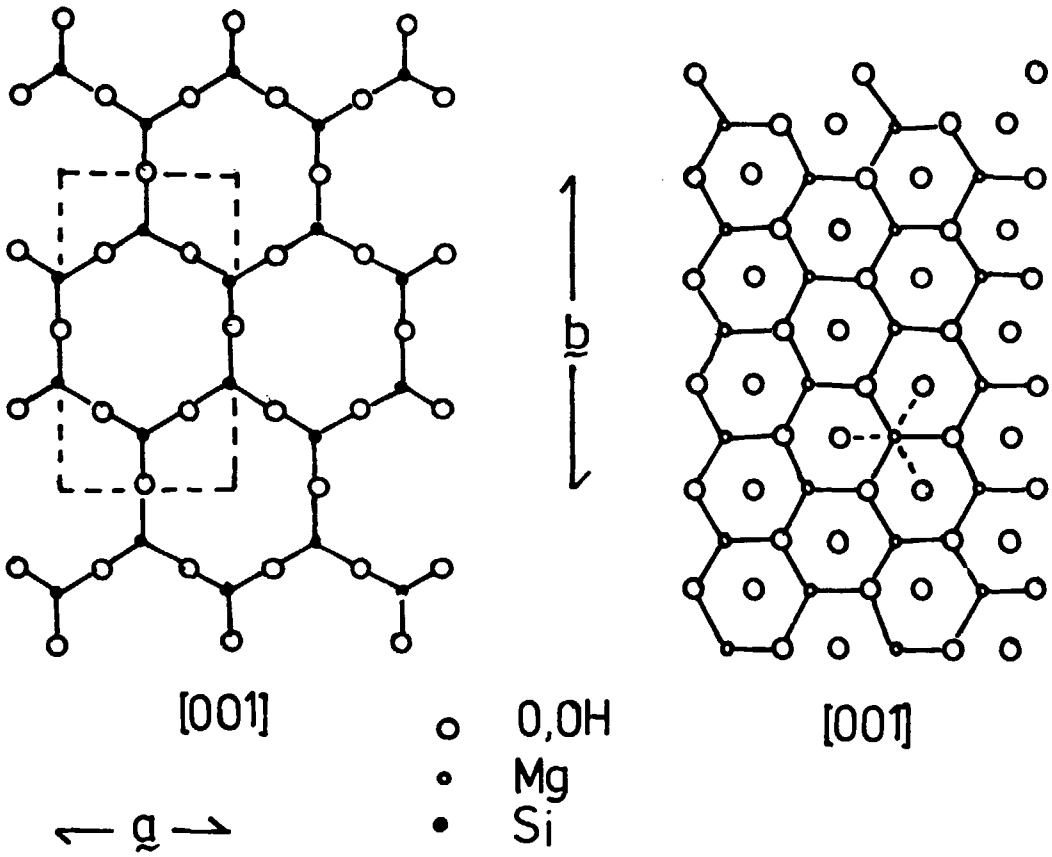

Fig 2

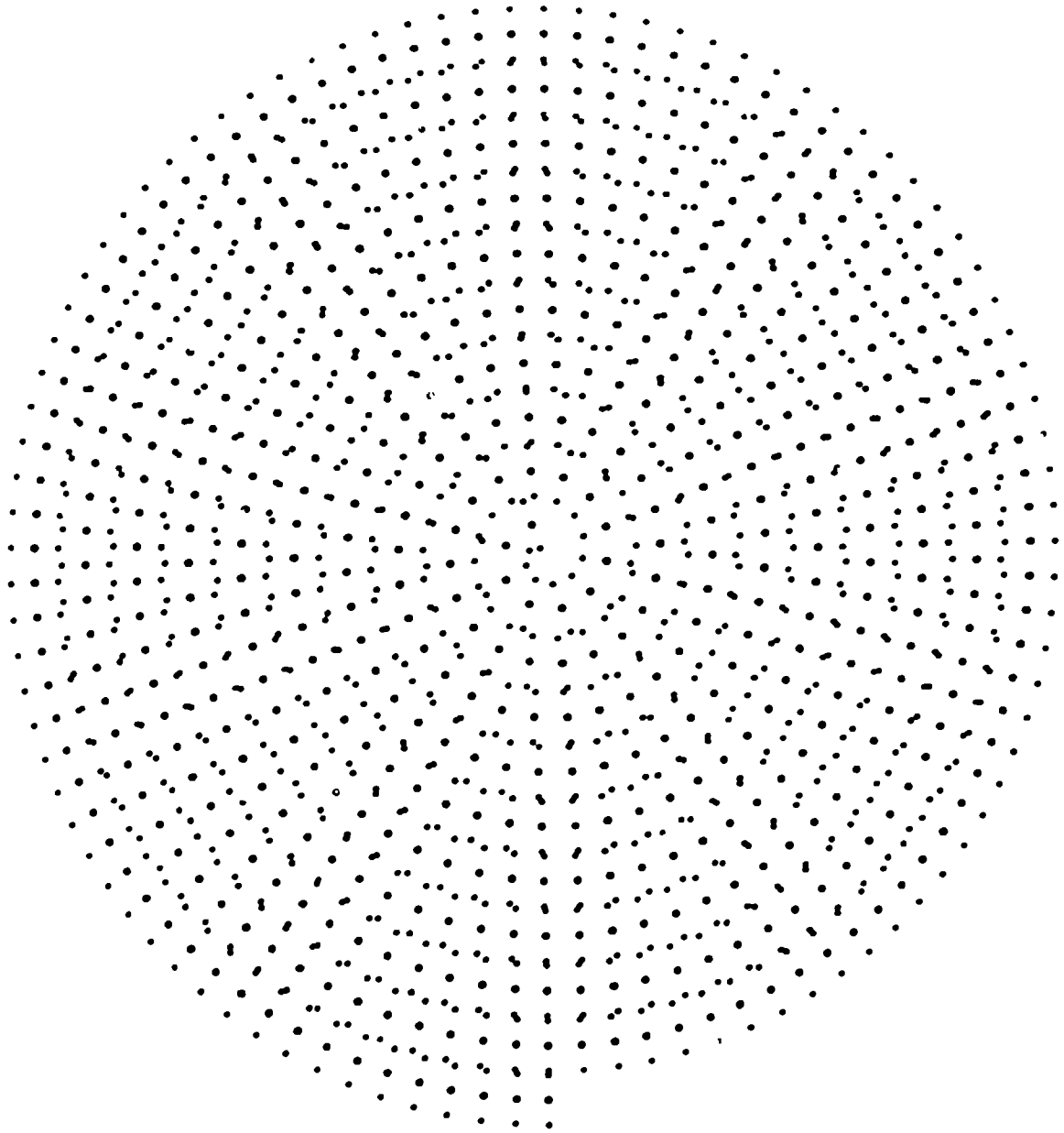

Fig 3

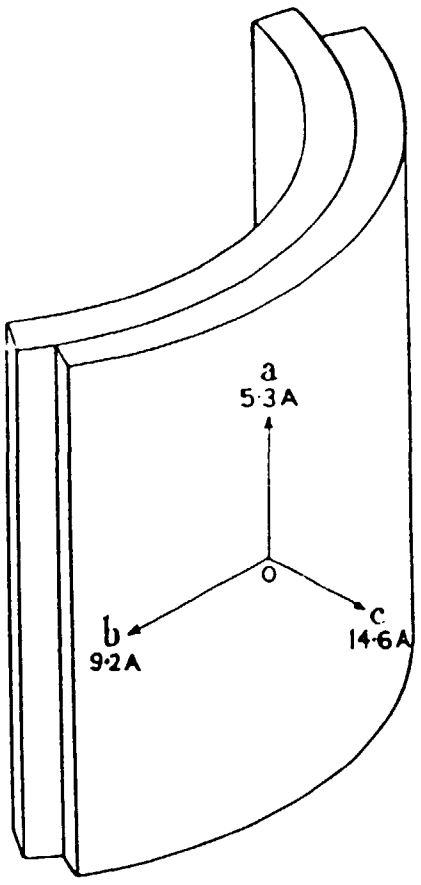

a

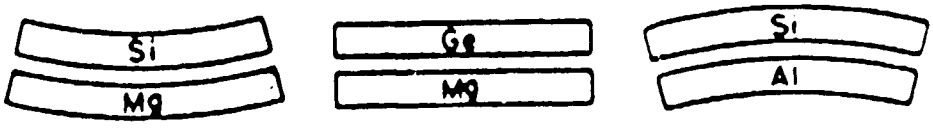

b

Fig 4

Fig 5a

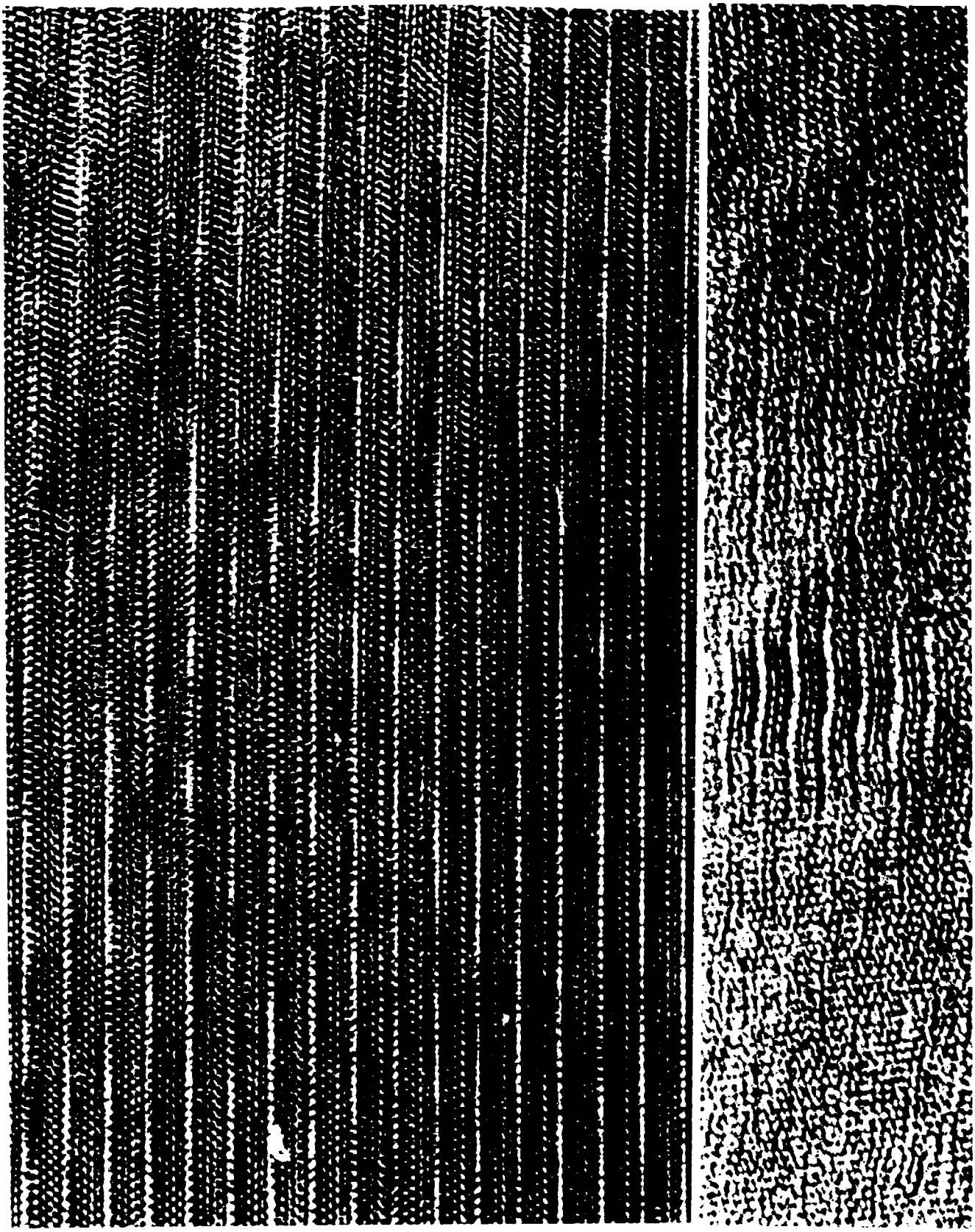

Fig 5

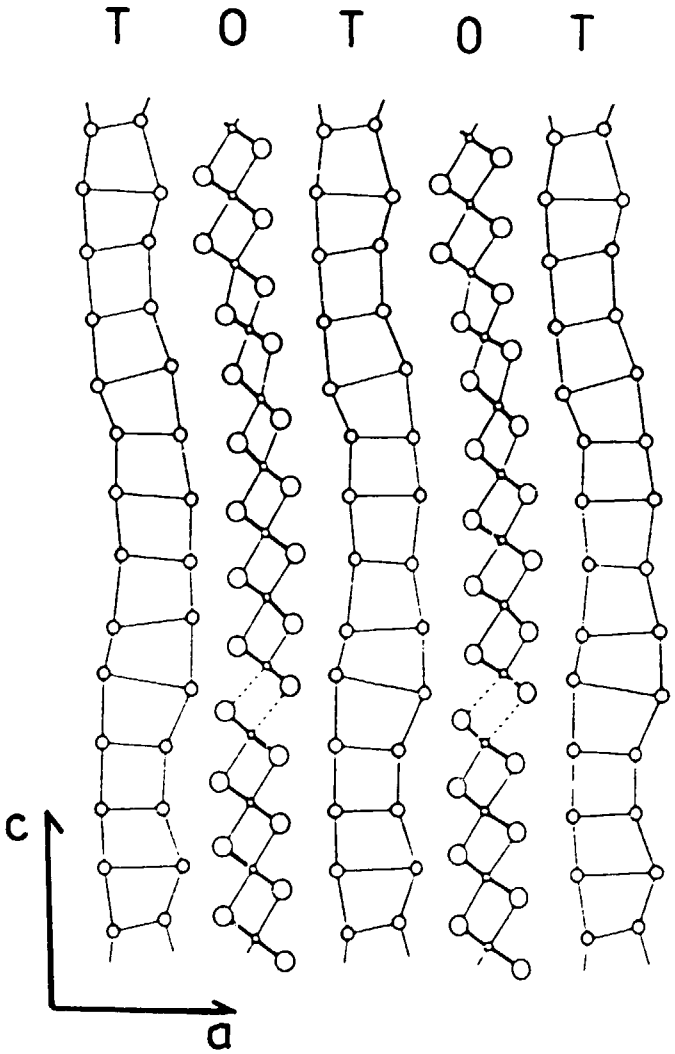

Fig 5d

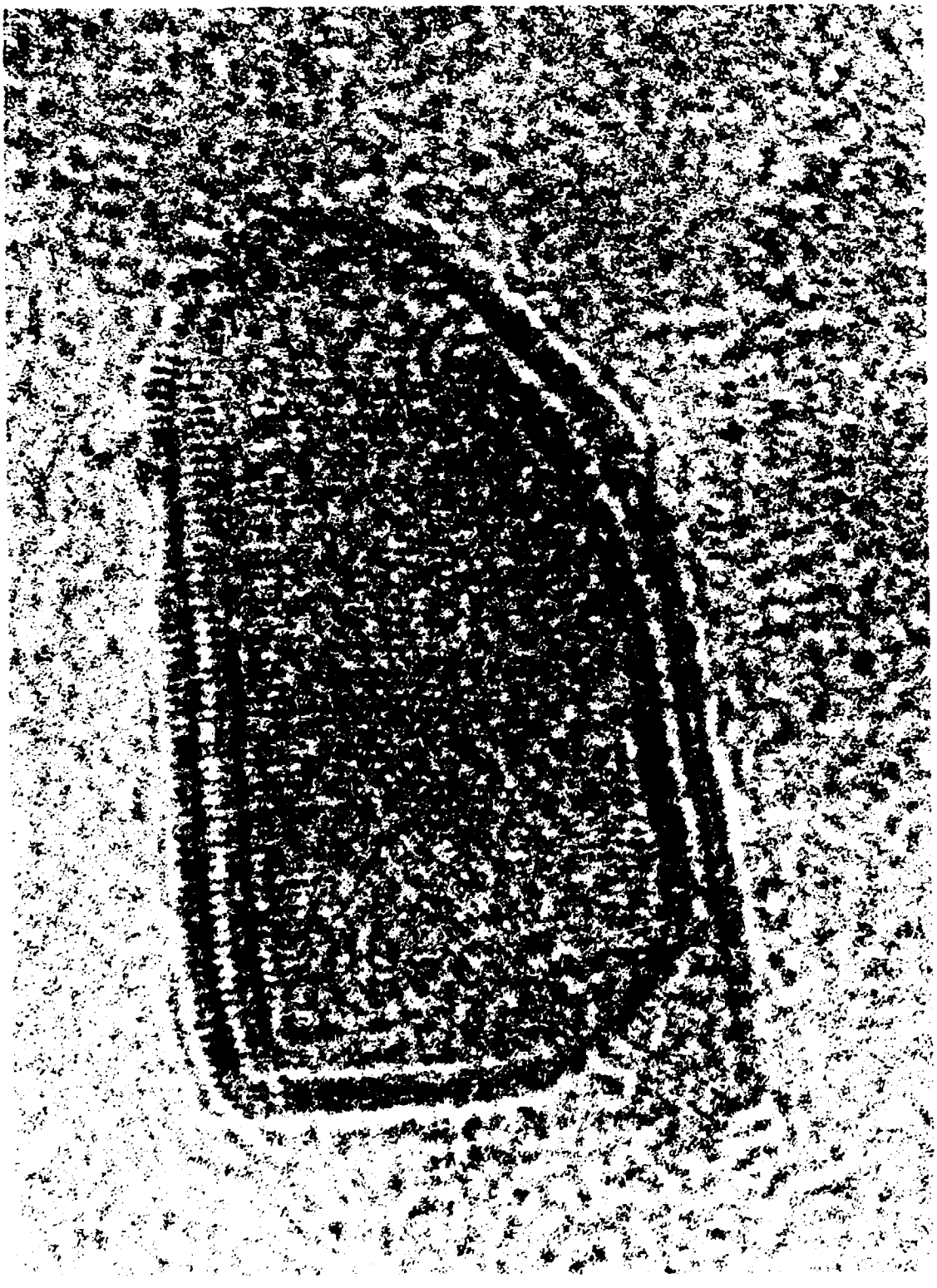

Fig 6a

Fig 6b

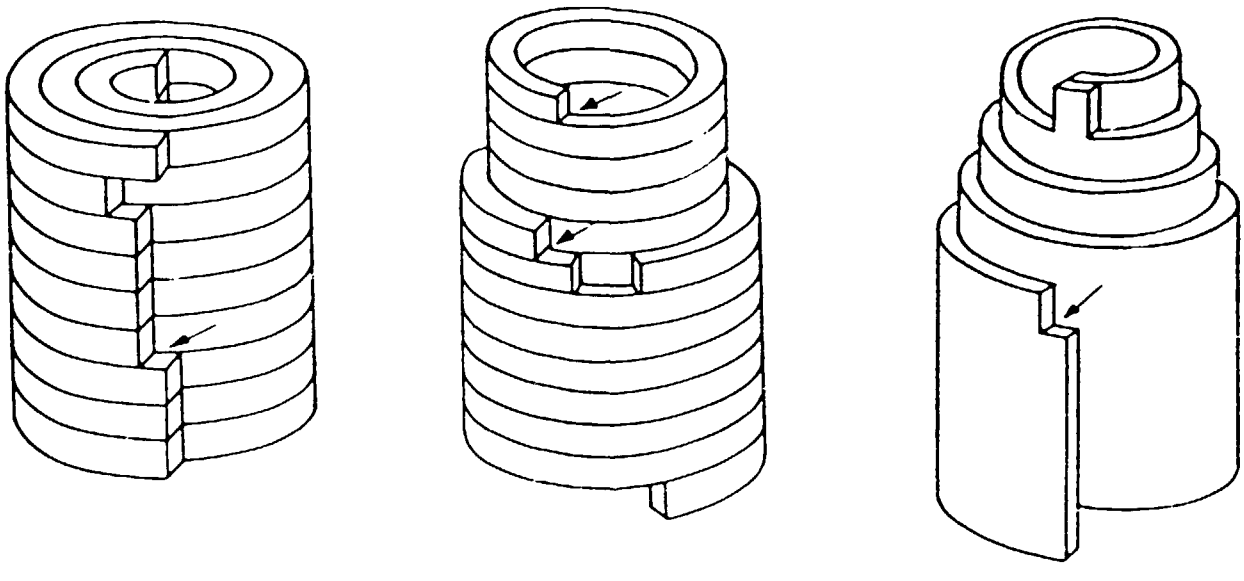

a b c

Fig 7

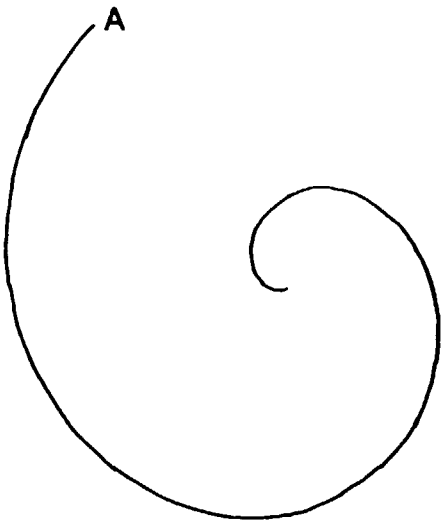

a

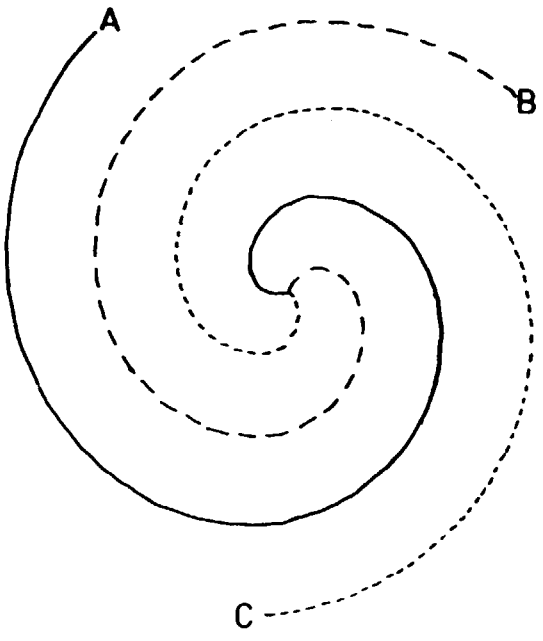

c

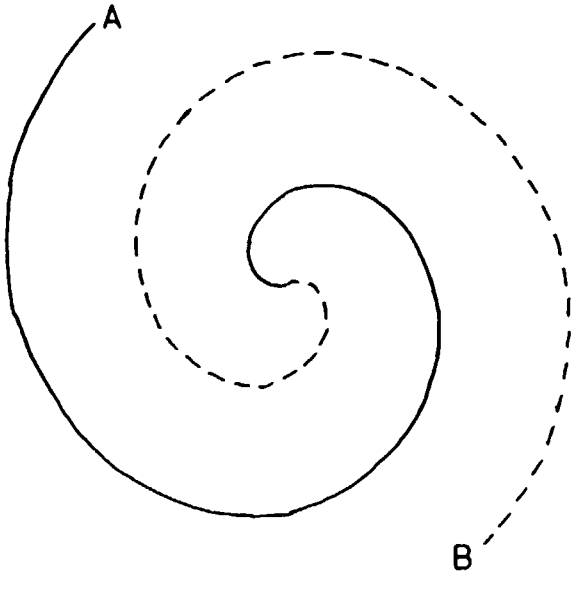

b

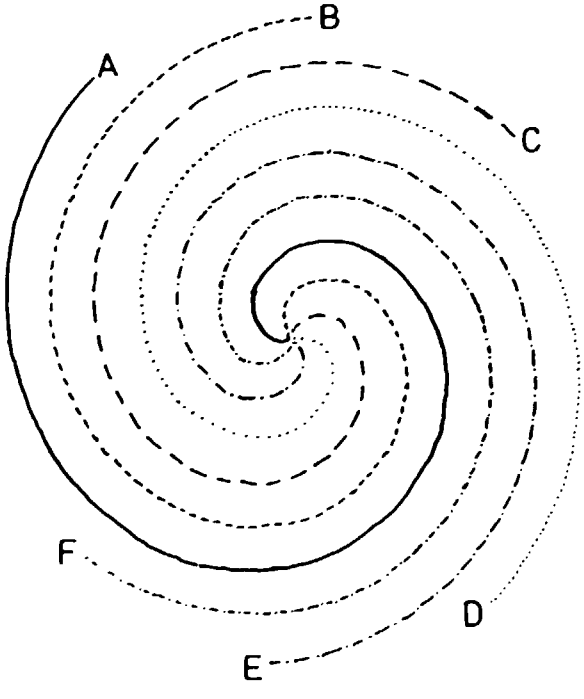

d

Fig 8